

Document downloaded from:

<http://hdl.handle.net/10251/68180>

This paper must be cited as:

García Pérez, JV.; Ozuna López, C.; Ortuño Cases, C.; Carcel Carrión, JA.; Mulet Pons, A. (2011). Modeling Ultrasonically Assisted Convective Drying of Eggplan. *Drying Technology*. 29(13):1499-1509. doi:10.1080/07373937.2011.576321.



The final publication is available at

<https://dx.doi.org/10.1080/07373937.2011.576321>

Copyright Taylor & Francis

Additional Information

12 ABSTRACT

13 In order to analyze the influence of ultrasound in mass transfer phenomena during
14 drying, modeling constitutes a fundamental tool. In this work, the study of the effect of
15 power ultrasound application on drying kinetics of eggplant was addressed by using
16 different models based on theoretical (diffusion) or empirical approaches. Drying kinetics
17 of eggplant cylinders (height 20 mm and diameter 24 mm) were carried at 40 °C and 1
18 m/s applying different ultrasonic power levels: 0, 6, 12, 19, 25, 31 and 37 kW/m³.
19 Experiments were carried out, at least, in triplicate for the different powers. Furthermore,
20 shrinkage and sorption isotherms were also addressed in order to reach an optimal
21 description of eggplant drying.

22 Drying kinetics were sped up by the ultrasonic application, moreover, the higher the
23 applied ultrasonic power the higher drying rate. A significant ($p < 0.05$) influence of the
24 ultrasonic power in both effective moisture diffusivity and mass transfer coefficient was
25 identified; which was well explained by linear relationships. The most complex model,
26 which considered external resistance, as well as shrinkage, as significant phenomena,
27 showed the best agreement with experimental data, providing percentages of explained
28 variance higher than 99.9% and mean relative errors lower than 1.2% in all the cases.
29 According to these results, ultrasound could be considered a potential technology to
30 improve the convective drying of eggplant.

31

32 *Keywords:* dehydration, ultrasound, mass transfer, diffusion, shrinkage.

33

34

35 INTRODUCTION

36 The energy consumption in food processing industries represents one of the largest
37 costs in the production, provoking the increase of the product price and a negative
38 environment impact. In developed countries, around of 12-25 % of the overall industrial
39 energy consumption is attributed to the drying industry (Mujumdar, 2007). At industrial
40 scale, the air-forced or convective drying is the most common way for dehydration. The
41 low kinetics during the falling rate period, which results in high energy consumption
42 (Chou and Chua, 2001), and the quality loss of the final product due to the high
43 temperatures employed (Lewicki et al., 2006) constitute the main limitations of
44 convective drying. Convective drying affects the biochemical properties of foodstuffs,
45 such as the deterioration of aroma compounds (Timoumi et al., 2006), the degradation of
46 nutritional substances (Santos and Silva, 2009), the browning reaction and the color loss
47 (Suvarnakuta et al., 2005). Other effects are linked to the variation of the volume or
48 shrinkage that is related with the volume of removed water, the mobility of the solid
49 matrix and the drying rate (Mayor and Sereno, 2004), it is responsible for the main
50 changes on mechanical properties of the product such as texture and rehydration
51 capability (Abasi et al., 2009).

52 As a consequence, the food industry has been seeking for new technologies not only
53 to improve the energy efficiency but also the quality of the dry products (Chou and Chua,
54 2001). In this sense, combining traditional methods with non-conventional energy sources
55 seems to be a sound way to improve drying processes. Power ultrasound has the
56 advantage over other technologies, such as microwave, infrared radiation and radio
57 frequency, of increasing the drying rate with a small heating effect, thus the influence on
58 mass transfer is related with mechanical and not heating mechanisms (Gallego-Juárez,
59 2010; De la Fuente et al., 2006). Literature reports that the application of power
60 ultrasound during convective drying influences on external and/or internal resistance to

61 mass transfer (García-Perez et al., 2009). Ultrasound brings about the reduction of
62 boundary layer by mechanical effects, such as pressure variations, oscillating velocities
63 and microstreaming that the ultrasonic waves introduce in the solid-gas interfaces. In
64 addition, ultrasound may also affect internal water transfer by the well-known “sponge
65 effect” (Mulet et al., 2010; Gallego-Juárez, 2010), the alternating expansions and
66 compressions waves induced in the material creates micro-channels suitable for liquid
67 movement (Mulet et al., 2010). In addition, the effects linked to the ultrasonic waves like
68 the cavitation (Gallego-Juárez, 2010; De la Fuente et al., 2006), may facilitate of the
69 removal of water molecules strongly attached in the solid matrix.

70 The application of power ultrasound in solid-gas processes is less frequent than in
71 solid-liquid due to the high impedance mismatch between the application systems and air,
72 and the high acoustic energy absorption of this medium (Mulet et al., 2010). Recent
73 advantages in the design and construction of new air borne ultrasonic transducers have
74 opened a broad interest on its use on convective drying. These transducers attain an
75 efficient energy transfer due to a power impedance mismatch with the air, large
76 amplitudes of vibration, high directionality, high power capacities and large radiating
77 areas (Gallego-Juárez, 2010). Previous works with carrot and lemon peel (García-Pérez et
78 al., 2009) have related the efficiency of the ultrasonic application with the properties of
79 the raw material to be dried. In this sense, the study of the ultrasound application on a
80 product with a highly unconsolidated porous structure like eggplant would be interesting
81 for analyze and quantify the ultrasound effects on drying process. Hence, in order to
82 properly evaluate and design a specific ultrasonic application for a product it results
83 convenient to address thoroughly the influence of ultrasound on the drying kinetics
84 (García-Pérez et al., 2009).

85 Modeling constitutes an approach for analyzing drying processes; both the water
86 equilibrium and the kinetics should be addressed. Water sorption isotherm shows the

87 relationship between the water activity and the equilibrium moisture content. A proper
88 mathematical description of the isotherms is needed in order to thoroughly address the
89 drying kinetic modeling, being the GAB model the most common equation to be used
90 (García-Pérez et al., 2008). There are empirical models, such as the Weibull (Cunha et al.,
91 1998) model, these models do not provide a physical description of the process but rather
92 give an outline of what happen and allow the identification of the most relevant variables.
93 (Mulet, 1994). In this sense, the Weibull model has been used for modeling drying
94 kinetics of different kind of foods (Azzouz et al., 2002, Simal et al., 2005). Other models
95 look for a better description like the diffusion models, based on the Fick's law (Crank,
96 1975), are built according to some assumptions which establish the degree of complexity
97 for the resolution. The most common assumptions to consider are related to the effective
98 moisture diffusivity (Maroulis et al., 2001), the external resistance to mass transfer (Simal
99 et al. 2003) and the food shrinkage (Mayor and Sereno, 2004). The analysis of the
100 influence on model behavior of assumption related to effective diffusivity or external
101 resistance are often addressed although shrinkage is seldom considered. The importance
102 of including the food shrinkage as a significant phenomenon in modeling has been widely
103 discussed in literature (Queiroz and Nebra, 2001; Hassini et al., 2007). Shrinkage, which
104 is linearly related to water content at the early stages of drying, is extremely important in
105 diffusion mechanisms during drying because it leads to a variation in the distance required
106 for the mobility of water molecules (Hernández et al., 2000). This phenomenon should be
107 included in the development of a model in order to improve the physical representation of
108 the process and to increase the validity of the effective diffusion coefficient (Queiroz and
109 Nebra, 2001). Therefore, in this work, shrinkage is an important variable during drying
110 modeling due to the shrinkage of eggplant is very remarkable and the reduction in sample
111 volume is larger than the volume of removed water due to its high porosity (Souma et al.,
112 2004).

113 The main aim of this work was to model the ultrasonic assisted drying kinetics of
114 eggplant under different experimental conditions considering different models based on
115 theoretical (diffusion) or empirical approaches. Drying modeling will allow gaining
116 insight into the effects of power ultrasound on drying process, as well as, quantifying
117 those effects.

118

119 **MATERIALS AND METHODS**

120 **Ultrasonic assisted drying kinetics**

121 Drying experiments were carried out using eggplants (*Solanum melongena* var Black
122 Enorma) purchased in a local market. For testing, cylinders (height 20 mm and diameter
123 24 mm) were taken from flesh of the eggplant using a houseware tool. The experiments
124 were conducted at 40 °C and 1 m/s applying seven ultrasonic power levels (UP): 0, 6, 12,
125 19, 25, 31, 37 kW/m³ until sample weight loss reached 75 %. Ultrasonic power was
126 defined as the electric power supplied to the ultrasonic transducer divided by the drying
127 chamber volume. For each condition tested, drying experiments were carried out at least
128 in triplicate. Drying kinetics were determined from the sample weight loss during drying
129 and the initial moisture content (AOAC, 1997).

130 For this purpose, a convective drier assisted by power ultrasound already described in
131 previous works (García-Pérez et al., 2006) was used. The drying chamber consist of an
132 aluminum vibrating cylinder (internal diameter 100 mm, height 310 mm and thickness 10
133 mm) driven by a piezoelectric composite transducer (21.8 kHz). The ultrasonically
134 activated drying chamber is able to generate a high-intensity ultrasonic field in its inside
135 reaching an average sound pressure of 154.3 dB (measured applying an electrical power
136 to the transducer of 75 W at air stagnant conditions). The equipment uses a pneumatic
137 device for weighting the samples at preset times and an impedance matching unit that

138 permits to fit the impedance output of the generator to the transducer providing a better
139 electric yield on the system.

140

141 **Sorption isotherm**

142 Fresh eggplant samples were dried for different times (from 4 to 48 h) in order to
143 obtain samples with different moisture content at 40 °C using an air forced tray oven. Dry
144 samples were milled and put in a hermetic glass container for 24 hours to facilitate that
145 the samples reached homogeneous moisture content. Thereafter, the water activity was
146 measured at 40 °C using an electric hygrometer (Model AW SPRINT TH500,
147 NOVASINA, Air Systems for Air Treatment, Pfäffikon, Switzerland), which was
148 previously calibrated using the followings salts: LiCl, MgCl₂, Mg(NO₃)₂, NaCl, BaCl₂
149 and K₂Cr₂O₇, according to the manufacturer guidelines. Finally, moisture content was
150 measured in each sample by using the AOAC method already mentioned. Thus, around 40
151 water activity-moisture content experimental points were obtained.

152 Sorption isotherm of eggplant were modeled using the GAB (Guggenheim-Anderson-
153 De Boer) model (Eq. 1), describing the moisture content as a function of water activity.

$$154 \quad W = W_m \frac{CKa_w}{(1 - Ka_w)(1 + (C - 1)(Ka_w))} \quad (1)$$

155 The identification of GAB model parameters (W_m , C and K) were carried out using an
156 optimization procedure that minimized the sum of the squared difference between
157 experimental and calculated average moisture content of samples. For that purpose, the
158 non linear optimization algorithm of the generalized reduced gradient (GRG), available in
159 Microsoft Excel™ spreadsheet from MS Office 2007 was used.

160

161 **Shrinkage measurement**

162 Cubic-shaped eggplant samples (side 18 mm) were used to determinate the change of
163 sample volume during drying. Cubes were dried at 40 °C and 1 m/s for different times:
164 0.5, 1, 2, 4 and 6 hours. Moisture content (AOAC method N° 934.06), and volume was
165 measured for estimating shrinkage. The volume measurement was performed
166 simultaneously by two different methodologies: image analysis and liquid displacement.
167 For image analysis, digital images were taken (DSC-P100, Sony Corp. Japan) for each
168 face of fresh and dehydrated samples. The area of these surfaces was estimated using the
169 software Sigma Scan Pro 5 (SPSS Inc., USA). The measurement was carried out in pixels
170 and afterwards converted in length. From this measurement, the volume was calculated
171 assuming samples did not lose the cubic shape during drying. The volume measurement
172 by liquid displacement was carried out with toluene (density 0.867 g/mL at 20 °C) a
173 volumetric standard picnometer (48.89 ml), and an analytical balance (PB 303-S, Mettler
174 Toledo). The shrinkage measurement was carried out in triplicate, at least, in 5 samples
175 for the different drying times.

176

177 **Modeling drying kinetics**

178 For analyzing the influence of power ultrasound on drying kinetics of eggplant
179 cylinders, three diffusion models based on the 2nd Fick's law with different degree of
180 complexity and one empirical model (Weibull) were used.

181

182 **Diffusion models**

183 The differential equation for diffusion is obtained combining Fick's law and the
184 microscopic mass balance. For isotropic solids and finite cylinder geometry, the diffusion
185 equation for expressed as follows considering a constant effective moisture diffusivity
186 (Eq. 2):

$$187 \quad \frac{\partial W_p(x, r, t)}{\partial t} = D_e \left(\frac{\partial^2 W_p(x, r, t)}{\partial x^2} + \frac{\partial^2 W_p(x, r, t)}{\partial r^2} + \frac{1}{r} \frac{\partial W_p(x, r, t)}{\partial r} \right) \quad (2)$$

188 In Eq. 2, the solid symmetry, and a uniform initial moisture content and temperature
 189 were considered as boundary and initial conditions, other boundary conditions are given
 190 in Table 1. For solving the diffusion equation different models were tested according to
 191 the 2nd boundary condition (Table 1) used to describe the properties of the gas-solid
 192 interface ($x=L$ or $r=R$) and also considering the change of sample volume during drying.
 193 This strategy allowed testing the ability and reliability of describing the drying kinetics
 194 using different assumptions.

195

196 **Negligible external resistance model (NER)**

197 The simplest diffusion model neglected the external resistance to mass transfer, thus,
 198 the water transfer is entirely controlled by water diffusion (Eq. 6 and Eq. 7, Table 1). The
 199 analytical solution (Crank, 1975) of the governing equation (Eq. 2) for NER model is
 200 showed in Eq. 11 in terms of the average moisture content.

$$201 \quad \psi(t) = \frac{W(t) - W_e}{W_0 - W_e} = \left[\sum_{n=0}^{\infty} \frac{8}{(2n+1)^2 \pi^2} e^{\left(-\frac{D_e (2n+1)^2 \pi^2 t}{4L^2} \right)} \right] \cdot \left[\sum_{n=1}^{\infty} \frac{8}{\alpha_n^2} e^{\left(-\frac{D_e \alpha_n^2 t}{R^2} \right)} \right] \quad (11)$$

202

203 **Model considering external resistance (ER)**

204 This model considers significant both internal and external resistance to moisture
 205 transport (Hernández et al., 2000). This fact was considered in the model through the
 206 boundary conditions stated in Eq. 8 and Eq. 9 (Table 1). A finite difference method was
 207 used to solve the ER model. For that purpose, the original volume of cylindrical samples
 208 was divided into a constant number of elements (20x20) that constituted the subvolumes
 209 network. According to this method, the local moisture content for a subvolume is obtained

210 as a function of the moisture content of the surrounding subvolumes and of the same
 211 subvolume at a given time (Eq. 12). From Eq. 12, the particular equation for each specific
 212 subvolume must be obtained by combining the particular boundary conditions.

$$\begin{aligned}
 &W_p(r, x, t-1) = \frac{D_e \Delta t}{\Delta x^2 + \Delta r^2} \times \\
 &\times \left[\begin{aligned}
 &W_p(r, x, t) \left(\left(\frac{\Delta x^2 + \Delta r^2}{D_e \Delta t} \right) + 2(\Delta x^2 + \Delta r^2) \right) - \\
 &\left(\begin{aligned}
 &W_p(r, x + \Delta x, t) \Delta r^2 + W_p(r, x - \Delta x, t) \Delta r^2 + \\
 &+ W_p(r + \Delta r, x, t) \Delta x^2 \left(1 + \frac{\Delta r}{2r} \right) + \\
 &+ W_p(r - \Delta r, x, t) \Delta x^2 \left(1 - \frac{\Delta r}{2r} \right)
 \end{aligned} \right) \right] \quad (12)
 \end{aligned}
 \end{aligned}$$

214 The position of the subvolume in the radial direction is characterized by the r
 215 parameter, the characteristic dimensions of the subvolume was determinate by $\Delta r = r/(n-1)$
 216 and $\Delta x = L/(n-1)$, the number of nodes in r or x direction by n (20) and, finally, the time
 217 interval considered by Δt (Cárcel et al., 2007). For solving the set of implicit equation of
 218 the network a program using Matlab® 7.1 SP3 (The MathWorks, Inc., Natick, MA, USA)
 219 was developed. This program calculated the moisture distribution inside a finite length
 220 cylindrical body and the average moisture content of the solid as a function of the drying
 221 time, the effective moisture diffusivity and the mass transfer coefficient.

222

223 **Model considering external resistance and shrinkage (ERS)**

224 The most complex diffusion model tested considered not only the external resistance
 225 to mass transfer but also the sample shrinkage as a significant phenomenon effecting both
 226 axial and radial directions during drying (Mayor and Sereno, 2004). In this case, mass
 227 transport was addressed as a moving boundary problem (Table 1).

228 Like in the ER model, the diffusion model was solved applying an implicit finite
 229 difference method using MATLAB. In this case, the subvolumes size is reduced due to

230 the sample's shrinkage adjusting its dimension on the moving boundary, remaining the
231 dry matter at a constant value during the process.

232

233 **Empirical model**

234 The empirical model of Weibull (Cunha et al., 1998) was used to compare its results
235 with the theoretical models (Eq. 13).

$$236 \quad W = W_e + (W_c - W_e) \cdot \exp\left(-\left(\frac{t}{\beta}\right)^\alpha\right) \quad (13)$$

237 Where α and β are the shape and kinetic parameters of the model, respectively. The β
238 parameter is inversely linked to drying rate. This parameter includes all the effects of the
239 process variables (temperature, air velocity and particle size) on the drying kinetics
240 (Blasco et al., 2006), thus, it is expected on influence of power ultrasound on this
241 parameter.

242

243 **Parameter estimation**

244 The identification of Weibull parameters (α and β) and NER model (D_e) were carried
245 out using an optimization procedure that minimized the sum of the squared difference
246 between experimental and calculated average moisture content of samples. For that
247 purpose, the non linear optimization algorithm of the generalized reduced gradient
248 (GRG), available in Microsoft Excel™ spreadsheet from MS Office 2007 was used.

249 In the case of ER and ERS models, the effective moisture (D_e) and the mass transfer
250 coefficient (k) were simultaneously identified using the SIMPLEX method available in
251 MATLAB (*fminsearch* function). The objective function minimized the sum of the
252 squared differences between the experimental and calculated average moisture content.

253

254 **Model fitting evaluation and statistical analysis**

255 The percentage of explained variance (% var) and the mean relative error (% MRE)
 256 (Lypson & Sheth 1973) were computed for evaluating the fit of the models to the
 257 experimental data (Eq. (14) and Eq. (15)).

$$258 \quad \% \text{VAR} = \left[1 - \frac{S_{xy}^2}{S_y^2} \right] \cdot 100 \quad (14)$$

$$259 \quad \% \text{MRE} = \frac{100}{N} \left[\sum_{i=1}^N \frac{|W_{ei} - W_{ci}|}{W_{ei}} \right] \quad (15)$$

260 In order to evaluate the significance of the differences between the identified
 261 parameters, the analysis of variance (ANOVA) was carried out and the LSD (least
 262 significant difference) intervals were identified. The statistical analysis was carried out
 263 using the Statgraphics Plus 5.1 software package (Statistical Graphics Corp., Herdorn,
 264 Virginia USA).

265

266 **RESULTS AND DISCUSSION**

267 **Sorption isotherm**

268 Experimental sorption isotherm and estimated curve with GAB model determined at
 269 40°C are shown in Fig. 1. The experimental data ranged between 2.679 and 0.044 (kg
 270 water/kg dry solid) for average moisture content and between 0.993 and 0.174 for water
 271 activity. The sorption isotherm of eggplant showed the typical sigmoid curve, according
 272 to BET classification (García-Pérez et al., 2008), look like a type III pattern. The
 273 parameters obtained by fitting water activity data to the GAB model (Eq. 1) were $W_m =$
 274 0.093 kg w/kg dry solid, $K = 0.99$ and $C = 3.01$. These values were used in drying kinetics
 275 modeling for calculating the equilibrium moisture content values (W_e) (NER model) and
 276 the local water activity in the sample surface (ϕ_e) (ER and ERS model).

277

278 **Eggplant shrinkage**

279 As can be observed in Fig. 2, eggplant sample volume was significantly reduced
 280 during drying process, thus, the lower the moisture content, the lower the volume. This
 281 fact has been also found in many vegetables, such as carrot, apple and potato (Mayor and
 282 Sereno, 2004; Hassini et al., 2007).

283 Image analysis and liquid displacement provided a similar pattern in shrinkage data,
 284 nevertheless, significant differences between both methods were observed at low moisture
 285 contents. Sample volume measured at low moisture contents using image analysis was
 286 significantly higher than the measured by liquid displacement. A significant ($p < 0.05$)
 287 linear relationship was established between the dimensionless volume and the moisture
 288 content for both shrinkage measurement methods.

$$289 \quad \frac{V}{V_0} = 0.929 \frac{W}{W_0} + 0.112; \quad R^2 = 0.99 \quad (16)$$

$$290 \quad \frac{V}{V_0} = 0.621 \frac{W}{W_0} + 0.309; \quad R^2 = 0.95 \quad (17)$$

291 A better correlation was found for liquid displacement (Eq. 16, $r^2 = 0.992$) than for
 292 image analysis data (Eq. 17, $R^2 = 0.953$). For that reason, shrinkage data obtained from
 293 liquid displacement analysis was chosen to be included in the ERS model. Using the
 294 liquid displacement methodology for evaluating the drying shrinkage, Souma et al.
 295 (2004), reported for eggplant cylinders slightly different linear equation coefficients,
 296 probably due to the different eggplant cultivar. Moreover, Wu et al. (2007) calculating an
 297 approximate volume and surface area of vacuum dried eggplant slab samples, found also
 298 linear equation coefficient values in the range of the obtained values in this work. These
 299 results points to a rather similar behavior independently of size, shape and cultivar.

300

301 **Experimental drying kinetics**

302 Experimental drying kinetics of eggplant cylinders at the different ultrasonic powers
303 are shown in Fig.3. The constant rate drying period was not observed in the drying
304 kinetics, thus, the average initial moisture content of eggplant (14.70 ± 0.17 kg water/kg
305 dry solid) was considered as the critical moisture content.

306 Experimental data showed a very intense effect of power ultrasound (Fig. 3). The
307 ultrasonic application sped up the drying kinetics. Thus, for reaching an average moisture
308 content of 2.9 kg water/kg dry solid, the application of the maximum ultrasonic power
309 tested (37 kW/m^3) reduced the drying time by approximately 72 % in comparison to the
310 experiments carried out without ultrasonic application (0 kW/m^3). The drying time
311 reduction induced by the ultrasonic application for eggplant was larger than for other
312 products. García-Pérez et al. (2009) using the same ultrasonic set-up and similar
313 experimental conditions found drying time reductions of 32 and 53 % in the drying of
314 carrot cubes and lemon peel slabs ($40 \text{ }^\circ\text{C}$ and 1 m/s), respectively. The intense effect of
315 power ultrasound on drying rate for eggplant may be linked to the material structure,
316 being the porosity one of the most important variables in determining the effectiveness of
317 the ultrasonic power on foodstuffs (García-Pérez et al., 2009). Hence, eggplant, which has
318 a tissue with a highly unconsolidated porous structure (Wu et al., 2007), may be
319 considered a more prone material to be affected by the ultrasonic energy than carrot and
320 lemon peel.

321

322 **Drying modeling**

323 For quantifying the influence of power ultrasound application on the mass transfer
324 process during the convective drying of eggplant cylinders, it is convenient to consider
325 modeling. In addition, modeling should be useful in order to establish the influence of
326 power ultrasound on external and internal mass transport. As already stated, theoretical
327 and empirical approaches for modeling the drying kinetics of eggplant will be evaluated.

328

329 **Non external resistance model (NER)**

330 The NER diffusion model described by Eq. 11 was used as a first approach for
331 modeling experimental drying kinetics of eggplant cylinders. The average effective
332 moisture diffusivity (D_e) identified from experimental results, the percentage of explained
333 variance (% VAR) and mean relative error (% MRE) obtained are shown in Table 2.

334 The identified effective moisture diffusivity ($3.31 \pm 0.37 \times 10^{-10} \text{ m}^2/\text{s}$) in the experiments
335 without ultrasound application ($0 \text{ kW}/\text{m}^3$) is similar to those estimated by different
336 authors for convective drying of eggplant and other foodstuffs at similar temperatures and
337 low drying air velocities. Chaves et al. (2003), reported a similar value ($2.93 \times 10^{-10} \text{ m}^2/\text{s}$)
338 for eggplant slices dried at $50 \text{ }^\circ\text{C}$. Queiroz and Nebra (2001), dried bananas ($29.9\text{-}68.4 \text{ }^\circ\text{C}$)
339 and found values of 1.25×10^{-10} to $7.64 \times 10^{-10} \text{ m}^2/\text{s}$. Sabarez and Price (1999), showed
340 effective diffusivity values around to $4.32\text{-}7.64 \times 10^{-10} \text{ m}^2/\text{s}$ for prunes dried at $70\text{-}85 \text{ }^\circ\text{C}$. In
341 these works a NER diffusion model was also used.

342 As observed in Table 2, the applied ultrasonic power during drying showed a
343 significant ($p < 0.05$) influence on the identified effective moisture diffusivity. Thus, the
344 maximum applied ultrasonic power level ($37 \text{ kW}/\text{m}^3$) increased the effective moisture
345 diffusion coefficient by 237 % in comparison to the identified value in the experiments
346 without power ultrasound application ($0 \text{ kW}/\text{m}^3$). The ultrasonic effects were dependent
347 on the power applied, the higher the applied ultrasonic power, the higher the identified
348 effective diffusivity values. In the range of the ultrasonic power level (UP) used in this
349 work ($0\text{-}37 \text{ kW}/\text{m}^3$), a significant ($p < 0.05$) linear relationship between the ultrasonic
350 power level and the effective moisture diffusivity was found (Fig. 4).

351 The improvement of the D_e values is associated with the mechanical effects brought
352 about by the ultrasonic application in the material being dried. The alternating expansions
353 and contractions cycles (“sponge effect”) may contribute to easy water leaving the solid

354 matrix thus reducing the internal resistance to mass transfer. García-Pérez et al. (2009)
355 reported an increasing of 40 % and 131 % in the identified effective diffusivity (using a
356 NER model) of carrot and lemon peel, respectively, when the same applied ultrasonic
357 power (37 kW/m^3) was tested. Previous results indicate that high porosity products are
358 more prone to the “sponge effect” showing a low internal resistance to the mechanical
359 stress; therefore, the effects of ultrasound should be more intense in this type of products
360 (García-Pérez et al., 2009).

361 The NER model provided low percentages of explained variance (ranged between 84-
362 87 %) and high percentages of the mean relative error (ranged between 16.5-18.5 %). The
363 poor fit of NER model may be linked to the boundary conditions proposed (Eq. 6 and Eq.
364 7, Table 1). Thus, the D_e values are simple fitting parameter, including not only the
365 diffusion mechanisms but also other mechanisms and phenomena not considered in the
366 modeling. In this sense, Akpinar and Bicer (2005) reported that at air velocities of 2.5 m/s
367 or lower, the external mass transport resistance is significant and needs to be considered
368 in the analysis of the eggplant drying data. Therefore, the use of a diffusion model
369 considering external resistance (ER model) would be necessary. In addition, as already
370 mentioned, the ER model will permit to separate external and internal resistance to mass
371 transfer.

372

373 **Model considering external resistance (ER)**

374 The ER model improved the description of the drying kinetics achieving percentages
375 of explained variance above 99 % and mean relative errors under 1.5 % in all the cases
376 (Table 3). Thus, considering the external resistance seems to be adequate in order to
377 describe the behavior of experimental eggplant drying.

378 The power ultrasound application affected the external resistance to water transport.
379 The mass transfer coefficient (k) was improved by 229 % when the maximum ultrasonic

380 power (37 kW/m^3) was applied. A similar effect was found for the effective diffusivity. A
381 significant ($p < 0.05$) linear relationship between the applied ultrasonic power level (UP)
382 and the effective diffusivity as well as the mass transfer coefficient (D_e and k) (Figs. 4 and
383 5) was also found in the range of the ultrasonic power level used in this work ($0\text{-}37$
384 kW/m^3).

385 Cárcel et al. (2007), in ultrasonic assisted drying of persimmon, reported an
386 improvement on the mass transfer coefficient of 34.5 % at 1 m/s and 31 kW/m^3 in
387 comparison to the experiments carried out without power ultrasound application. These
388 authors analyzed the influence of drying air velocity on the external mass transport
389 resistance during the ultrasonic drying and concluded that at low drying air velocities (< 4
390 m/s), the external resistance is significant and should be included in the modeling. The
391 increase of the mass transfer coefficient is linked to the reduction of the boundary layer
392 thickness due to different effects of ultrasound like pressure variations, oscillating
393 velocities and micro-streaming on the solid-gas interfaces. Therefore, these effects should
394 be the responsible of the reduction of the boundary layer of diffusion and as a
395 consequence, the improvement of the water transfer rate from the solid surface to the air
396 medium (Gallego-Juárez et al., 1999).

397 Although the ER model provides a good description of drying curves, it can be also
398 improved considering the shrinkage of the product as a phenomenon which would explain
399 better the dehydration process and also increasing the confidence on the identified
400 diffusion coefficient.

401

402 **Model considering external resistance and shrinkage (ERS)**

403 The most complex model showed high percentages of explained variance, in all the
404 cases higher than 99.9 %, and low percentages of mean relative error, less than 1.2 %
405 (Table 4). Both statistical parameters indicate a close fit between calculated and

406 experimental data, even better than the obtained in the ER model. The close fit confirms
407 that the assumption of significant external resistance and shrinkage considered in the
408 modeling seems to be adequate for eggplant drying process. Significant ($p < 0.05$) linear
409 relationships were found between mass transfer coefficient and effective moisture
410 diffusivity and the applied ultrasonic power (UP) (Figs.4 and 5).

411 As can be observed in Fig.4, when shrinkage is not included in modeling (ER model),
412 the values of D_e are overestimated in the range of 81.8-88.7 %. According to this
413 assumption, Rahman and Kumar (2007) analyzed the influence of shrinkage on effective
414 moisture diffusivity during drying of potato cylinders (length 50 mm and thickness of
415 5,8,10 and 16 mm) and slices (thickness 10 mm) and found overestimated D_e values in the
416 range of 75.9-128.1 % when shrinkage is not taken into account in the analysis. For
417 drying (29.9-68.4 °C) of banana, Queiroz and Nebra (2001), found overestimated D_e
418 values in the range of 20-50 %. Similar conclusions were also reported by Hernández et
419 al. (2000), during drying (50, 60 and 70 °C and 3 m/s) of mango (thickness 5, 10 and 15
420 mm) and cassava (thickness 10, 20 and 30 mm) slices. The overestimated values of
421 effective moisture diffusivity may be attributed to that the fact that shrinkage reduces the
422 distance for the diffusion of water molecules.

423 The mass transfer coefficients identified in the ERS model were slightly lower than in
424 the ER model but the differences were not significant (Fig. 5). The sample shape may
425 affect the water convective transport, but in this work, the inclusion of the shrinkage did
426 not provide differences in the mass transfer coefficient.

427

428 **Weibull model**

429 The Weibull model described adequately the drying kinetics at the different
430 experimental condition tested in this work. The percentages of explained variance (VAR)
431 were, in all cases, higher than 99.9 %, while the percentages of mean relative error (MRE)

432 were lower 1.1 % (Table 5). The value of the statistical parameters were similar to the
433 obtained using the ERS model. For real time applications the use of Weibull model maybe
434 advantageous due to its computational simplicity.

435 On the one hand, the shape parameter, α , was not dependent of the applied ultrasonic
436 power level. On the other hand, the kinetic parameter β decreased as the applied
437 ultrasonic power increased. As the β parameter is inversely proportional to drying rate, a
438 reduction of this value indicates an increase of the drying rate. A significant ($p < 0.05$)
439 linear relationship between the ultrasonic power level and $1/\beta$ was found in the range of
440 the ultrasonic power level used in this work (0-37 kW/m³) (Fig. 6). García-Pérez et al.
441 (2006) found a similar correlation in carrot cubes (18 mm) dried at 40 °C and 0.6 m/s.

442 Weibull model provides similar information than the diffusion models about the
443 influences of the ultrasonic power on the kinetic parameters. However, Weibull model has
444 two main limitations: its results cannot be extrapolated to other working conditions or
445 product geometries and does not provide information about mass transport mechanisms.
446 Notwithstanding, this empirical model may be used as a first approach to more complex
447 models, and also its use on further industrial applications may be considered relevant due
448 to its simplicity.

449

450 CONCLUSIONS

451 A diffusion model, considering external resistance to mass transfer and shrinkage to
452 be significant phenomena, provided a good description of eggplant drying kinetics. In
453 addition, it allows quantifying the ultrasonic effects on mass transport rate. The Weibull
454 empirical model also provides good results and could be useful for control purposes.
455 From the results obtained in this work, it is considered that power ultrasound has a high
456 potential application in drying processes due to the improvement on both internal and

457 external mass transport. Further research efforts are required in order to apply this
 458 technology at industrial scale.

459

460 **ACKNOWLEDGMENTS**

461 **PROMETEO Y MINISTERIO**

462

463 **NOMENCLATURE**

464

a_w	Water activity
C	GAB model parameter, dimensionless (Eq. 1)
D_e	Effective diffusivity, m^2/s
K	GAB model parameter, dimensionless (Eq. 1)
k	Mass transfer coefficient, $kg\ water/m^2/s$
L	Half height, m
R	Radius, m
r	Radial co-ordinate, m
S_y	Standard deviation of the sample
S_{yx}	Standard deviation of the estimation
T	Temperature, K
t	Time, s
W	Average equilibrium moisture content, $kg\ water/kg\ dry\ solid$
W_c	Critical moisture content, $kg\ water/kg\ dry\ solid$
W_{ci}	Calculated moisture content, $kg\ water/kg\ dry\ solid$
W_e	Equilibrium moisture content, $kg\ water/kg\ dry\ solid$.
W_{ei}	Experimental moisture content, $kg\ water/kg\ dry\ solid$

W_m	Monolayer average equilibrium moisture content, kg water/kg dry solid
W_p	Local moisture content, kg water/kg dry solid
x	Axial co-ordinate, m
α	Weibull model parameter, dimensionless
α_n	Eigenvalues
β	Weibull model parameter, s
ρ_{ss}	Dry solid density, kg/m ³
φ_{air}	Relative humidity drying air
φ_e	Water activity
ψ	Dimensionless moisture

465

466 **REFERENCES**

- 467 1. Mujumdar, A.S. An overview of innovation in industrial drying: current status and
468 R&D needs. *Transport in Porous Media* **2007**, *66*, 3-18.
- 469 2. Chou, S.K; Chua, K.J. New hybrid drying technologies for heat sensitive
470 foodstuff. *Trends in Food Science & Technology* **2001**, *12*, 359-369.
- 471 3. Lewicki P. P. Design of hot air drying for better foods. *Trends in Food Science &*
472 *Technology* **2006**, *17*, 153-163.
- 473 4. Timoumi, S.; Mihoubi, D.; Zagrouba, F. Shrinkage, vitamin C degradation and
474 aroma losses during infra-red drying of apple slices. *Swiss Society of Food*
475 *Science and Technology* **2006**, *40*, 1648-1654.
- 476 5. Santos, P.H.S; Silva, M.A. Kinetics of L-ascorbic degradation in pineapple drying
477 under ethanolic atmosphere. *Drying Technology* **2009**, *27*, 947-954.
- 478 6. Suvarnakuta, P.; Devahastin, S.; Mujumdar, A. S. Drying kinetics and β -carotene
479 degradation in carrot undergoing different drying processes. *Journal of Food*
480 *Science* **2005**, *70* (8), s520-s526.

- 481 7. Mayor, L.; Sereno, A.M. Modelling shrinkage during convective drying of food
482 materials: a review. *Journal of Food Engineering* **2004**, *61*, 373-386.
- 483 8. Abasi, S.; Mousavi, S. M.; Mohebi, M.; Kiani, S. Effect of time and temperature
484 on moisture content, shrinkage, and rehydration of dried onion. *Iranian Journal of*
485 *Chemical Engineering* **2009**, *6*(3), 57-60.
- 486 9. Gallego-Juárez, J.A. High power ultrasound processing: recent developments and
487 prospective advances. *Physics Procedia* **2010**, *3*, 35-47.
- 488 10. De la Fuente, S.; Riera, E.; Acosta, V.M.; Blanco, A.; Gallego-Juárez, J.A. Food
489 drying process by power ultrasound, *Ultrasonics* **2006**, *44*, e523-e527.
- 490 11. García-Pérez, J.V.; Cárcel, J.A; Riera, E.; Mulet A. Influence of applied acoustic
491 energy on the drying of carrots and lemon peel. *Drying Technology* **2009**, *27*, 281-
492 287.
- 493 12. Mulet, A.; Cárcel, J.A.; Sanjuan, N.; García-Pérez, J.V. Food dehydration under
494 forced convection conditions. In *Recent Progress in Chemical Engineering*;
495 Delgado J. (Ed.), Studium Press LLC; Houston, TX, USA. **2010**.
- 496 13. García-Pérez, J.V.; Cárcel, J.A.; Clemente, G.; Mulet, A. Water sorption isotherms
497 for lemon peel at different temperatures and isosteric heats. *LWT- Food Science*
498 *and Technology* **2008**, *41*, 18-25.
- 499 14. Cunha, L.M.; Oliveira, F.A.R.; Oliveira, J.C. Optimal experimental design for
500 estimating the kinetic parameters of processes described by the Weibull
501 probability distribution function. *Journal of Food Engineering* **1998**, *37*, 175-191.
- 502 15. Mulet, A. Drying modelling and water diffusivity in carrots and potatoes. *Journal*
503 *of Food Engineering* **1994**, *22*, 329-348.
- 504 16. Azzouz, S.; Guizani, A.; Jomaa, W.; Belghith, A. Moisture diffusivity and drying
505 kinetic equation of convective drying of grapes. *Journal of Food Engineering*
506 **2002**, *55*, 323-330.

- 507 17. Simal, S., Femenía, A.; Garau, M.C.; Rosselló, C. Use of exponential, Page's and
508 diffusional models to simulate the drying kinetics of kiwi fruit. *Journal of Food*
509 *Engineering* **2005**, *66*, 323-328.
- 510 18. Crank, J. *The Mathematics of Diffusion*; Oxford University Press, London, 1975.
- 511 19. Maroulis, Z.B.; Saravacos, G.D.; Panagiotou, N.M.; Krokida, M.K. Moisture
512 diffusivity data compilation for foodstuffs: effect of material moisture content and
513 temperature. *International Journal of Food Properties* **2001**, *4*, 225-237.
- 514 20. Simal, S.; Femenía, A.; García-Pascual, P.; Rosselló, C. Simulation of the drying
515 curves of a meat-based product: effect of the external resistance to mass transfer.
516 *Journal of Food Engineering* **2003**, *58*, 193-199.
- 517 21. Queiroz, M.R.; Nebra, S.A. Theoretical and experimental analysis of shapes of
518 selected vegetables materials on drying kinetics of bananas. *Journal of Food*
519 *Engineering* **2001**, *47*, 127-132.
- 520 22. Hassini, L.; Azzouz, S.; Peczalski, R.; Belghith, A. Estimation of potato moisture
521 diffusivity from convective drying kinetics with correction for shrinkage. *Journal*
522 *of Food Engineering* **2007**, *79*, 47-56.
- 523 23. Hernández J.A.; Pavón G.; García M.A. Analytical solution of mass transfer
524 equation considering shrinkage for modeling food-drying kinetics. *Journal of Food*
525 *Engineering* **2000**, *45*, 1-10.
- 526 24. Souma, S.; Tagawa, A. A.; Limoto, M. Structural properties for fruits and
527 vegetables during drying. *Journal of the Japanese Society for Food Science and*
528 *Technology* **2004**, *51(11)*, 577-584.
- 529 25. Association of Official Analytical Chemists. *Official Methods of Analysis*;
530 AOAC: Washington, DC, 1997.
- 531 26. García-Pérez, J.V.; Cárcel, J.A.; De la Fuente, S.; Riera, E. Ultrasonic drying of
532 foodstuff in a fluidized bed. Parametric study, *Ultrasonics* **2006**, *44*, e539-e543.

- 533 27. Cárcel, J.A.; García-Pérez, J.V.; Riera, E.; Mulet, A. Influence of high intensity
534 ultrasound on drying kinetics of persimmon, *Drying Technology* **2007**, *25*: 185-
535 193.
- 536 28. Blasco, M.; García-Pérez, J.V.; Bon, J.; Carreres, J.E.; Mulet, A. Effect of
537 blanching and air flow rate on turmeric drying. *Food Science and Technology*
538 *International* **2006**, *12*, 315-323.
- 539 29. Lypson, C.; Sheth, J.J. *Statistical Design and Analysis of Engineering*
540 *Experiments*; McGraw-Hill, New York, 1973.
- 541 30. Wu, L.; Orikasa, T.; Ogawa, Y.; Tagawa, A. Vacuum drying characteristics of
542 eggplant. *Journal of Food Engineering* **2007**, *83*, 422-429.
- 543 31. Chaves, M.; Sgroppo, S.C.; Avanza, J.R. *Cinéticas de secado de berenjena*
544 *(Solanum melongena L.)*. Comunicaciones Científicas y Tecnológicas.
545 Universidad Nacional del Nordeste, Argentina 2003.
- 546 32. Sabarez, H.T; Price, W.E. A diffusion model for prune dehydration. *Journal of*
547 *Food Engineering* **1999**, *42*, 167-172.
- 548 33. Akpınar, E.K.; Bicer, T. Modelling of drying of eggplants in thin-layers.
549 *International Journal of Food Science and Technology* **2005**, *40*, 273-281.
- 550 34. Rahman N.; Kumar S. Influence of shape size and shape on transport parameters
551 during drying of shrinking bodies. *Journal of Food Process Engineering* **2007**, *20*,
552 186-203.

553

554

1. TABLES

555

TABLE 1. Initial and boundary conditions for diffusion models considered for modeling drying kinetics of eggplant cylinders.

556

Models			Initial condition	Equation	External resistance	Sample volume
Common	t=0	0≤x≤L; 0≤r≤R	W _p (r,x,0)=W ₀	(3)		
Boundary conditions						
Common	t>0	r=0; 0≤x≤L	$\frac{\partial W_p(0,x,t)}{\partial r} = 0$	(4)		
	t>0	x = 0 ; 0 ≤ r ≤ R	$\frac{\partial W_p(r,0,t)}{\partial x} = 0$	(5)		
Negligible External Resistance (NER)	t>0	r = R ; 0 ≤ x ≤ L	W _p (R, x, t) = W _e	(6)	Negligible	Constant
	t>0	x = L ; 0 ≤ r ≤ R	W _p (r, L, t) = W _e	(7)		
External Resistance (ER)	t>0	r = R ; 0 ≤ x ≤ L	$-D_e \rho_{ds} \frac{\partial W_p(R, x, t)}{\partial r} = k(\varphi_e(R, x, t) - \varphi_{air})$	(8)	Significant	Constant
	t>0	x = L ; 0 ≤ r ≤ R	$-D_e \rho_{ds} \frac{\partial W_p(r, L, t)}{\partial x} = k(\varphi_e(r, L, t) - \varphi_{air})$	(9)		
External Resistance and Shrinkage (ERS)	t>0	r = R ; 0 ≤ x ≤ L	$-D_e \rho_{ds} \frac{\partial W_p(R, x, t)}{\partial r} = k(\varphi_e(R, x, t) - \varphi_{air})$	(10)	Significant	Variable L=f(W)

557 TABLE 2. NER model. Effective diffusivity (D_e). Percentage of explained variance (% VAR)
 558 and mean relative error (% MRE) identified from modeling. Subscripts (a,b,c,d) show
 559 homogeneous group established from LSD intervals ($p < 0.05$).

560

UP (kW/m ³)	D_e (10 ⁻¹⁰ m ² /s)	VAR (%)	MRE (%)
0	3.31±0.3 _a	85.9	16.5
6	4.26±0.8 _a	85.2	18.1
12	6.19±0.5 _b	85.8	18.1
19	6.31±0.2 _b	84.9	18.5
25	8.84±0.2 _c	86.7	17.3
31	9.14±1.0 _c	85.9	18.0
37	11.16±1.0 _d	86.8	16.8

561

562

563

564

565 TABLE 3. ER model. Effective diffusivity (D_e) and mass transfer coefficient (k). Percentage
 566 of explained variance (% VAR) and mean relative error (% MRE) identified from modeling.
 567 Subscripts (a,b,c,d,e,f) and (w,x,y,z) show homogeneous group established from LSD intervals
 568 ($p < 0.05$).

569

UP (kW/m ³)	D_e (10 ⁻¹⁰ m ² /s)	k (10 ⁻³ kg W/m ² /s)	VAR (%)	MRE (%)
0	8.9±1.0 _a	1.87±0.2 _w	99.9	0.9
6	11.8±2.7 _{ab}	2.32±0.4 _w	99.9	0.9
12	16.3±1.2 _{bc}	3.35±0.3 _x	99.9	0.7
19	17.8±4.1 _{cd}	3.43±0.3 _x	99.8	1.3
25	22.7±3.0 _{de}	4.86±0.2 _y	99.9	0.9
31	23.5±3.1 _{ef}	4.79±0.7 _y	99.9	1.0
37	27.9±3.6 _f	6.16±0.9 _z	99.8	1.4

570

571

572

573 TABLE 4. ERS model. Effective diffusivity, average of percentage explained and mean
 574 relative error. Subscripts (a,b,c,d) and (w,x,y,z) show homogeneous group established from
 575 LSD intervals ($p < 0.05$).

576

UP (kW/m ³)	D _e (10 ⁻¹⁰ m ² /s)	k (10 ⁻³ kg w/m ² /s)	VAR (%)	MRE (%)
0	4.9±0.1 _a	1.79±0.1 _w	99.9	0.4
6	6.3±1.4 _a	2.22±0.4 _w	99.9	0.5
12	8.9±1.8 _b	3.20±0.2 _x	99.9	0.6
19	9.4±1.7 _b	3.29±0.1 _x	99.9	1.0
25	12.3±1.4 _c	4.65±0.1 _y	99.9	0.9
31	12.7±1.7 _c	4.58±0.7 _y	99.9	0.5
37	15.2±1.8 _d	5.89±0.8 _z	99.9	1.1

577

578

579 Table 5. Weibull model. Parameters, α and β , percentage of explained variance and mean
 580 relative error. Subscripts (a,b,c,d,e) show homogeneous group established from LSD intervals
 581 ($p < 0.05$).

582

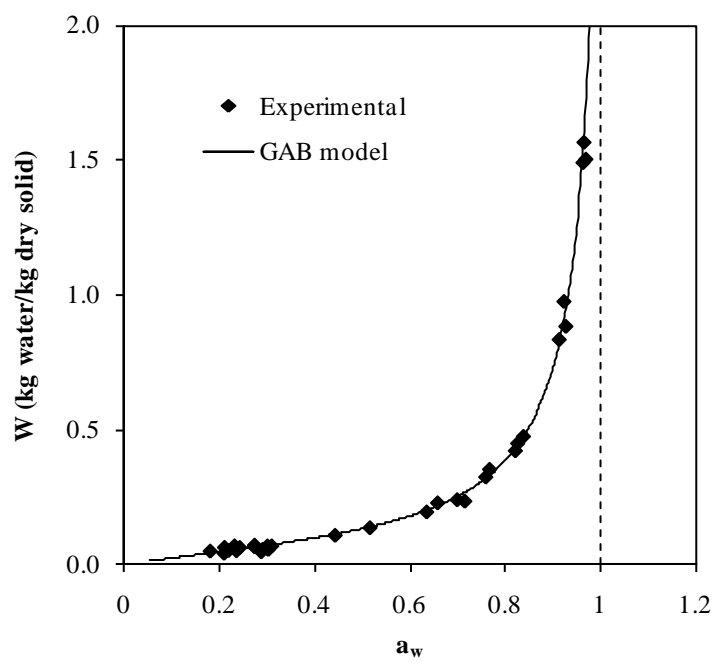
UP (kW/m ³)	β (10 ³ s)	α	VAR (%)	MRE (%)
0	15.30±0.8 _a	1.08±0.01	99.9	0.6
6	12.46±2.8 _a	1.11±0.02	99.9	0.6
12	8.51±0.7 _{ab}	1.09±0.02	99.9	0.5
19	8.21±0.6 _{bc}	1.11±0.10	99.9	0.7
25	5.96±0.3 _c	1.07±0.06	99.9	0.4
31	6.00±0.8 _d	1.10±0.03	99.9	0.6
37	4.80±0.6 _e	1.07±0.04	99.9	1.0

583

584

585 1. FIGURE CAPTIONS

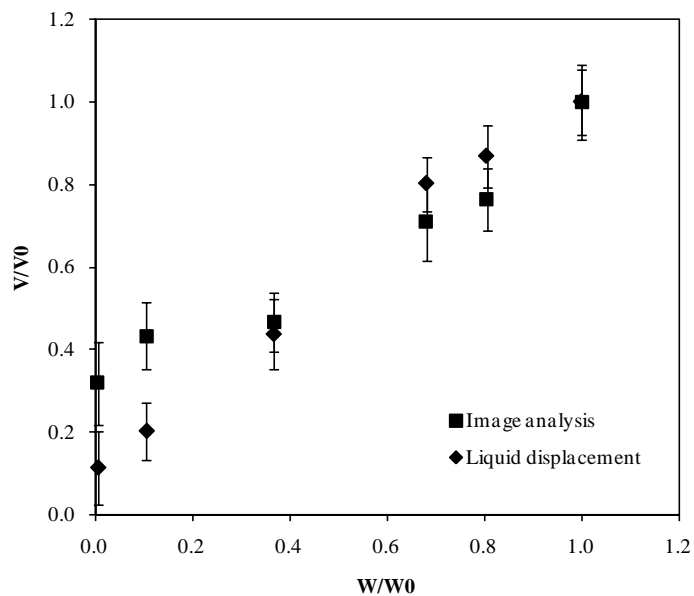
586



587

588 FIG.1. Experimental sorption isotherm and estimated curve with GAB model at 40 °C.

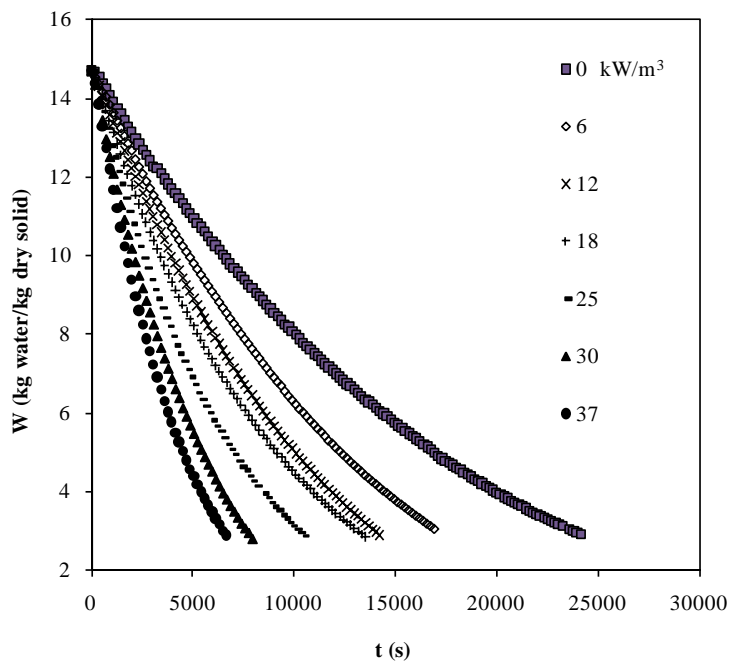
589



590

591 FIG. 2. Experimental shrinkage data for eggplant drying. V: Volume (m^3), W: Average
592 moisture content (kg water/kg dry solid), subscript 0: Initial. Standard deviation values.

593



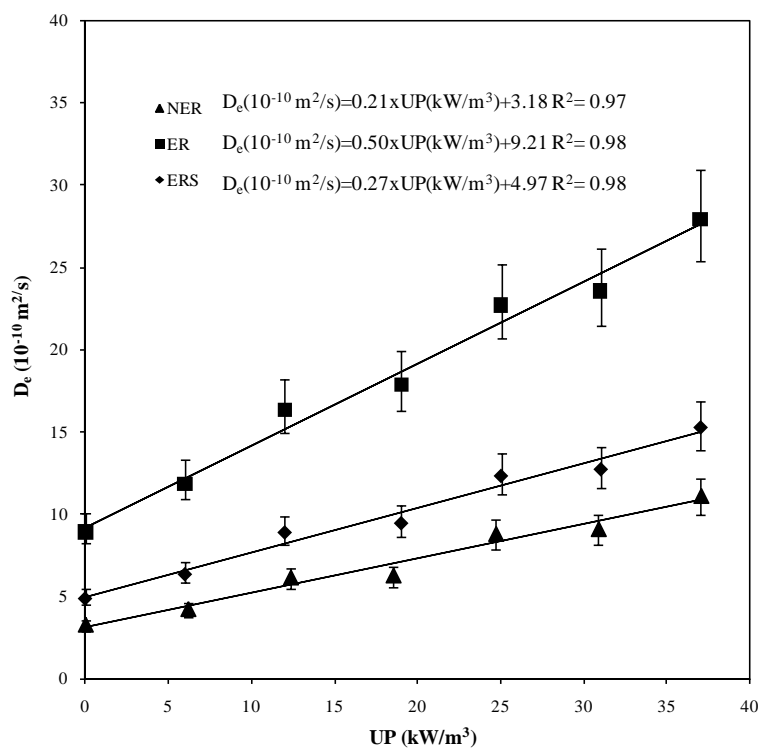
594

595

596 FIG 3. Drying kinetics of eggplant cylinders at 40°C and 1 m/s applying different ultrasonic
597 power levels (kW/m³).

598

599



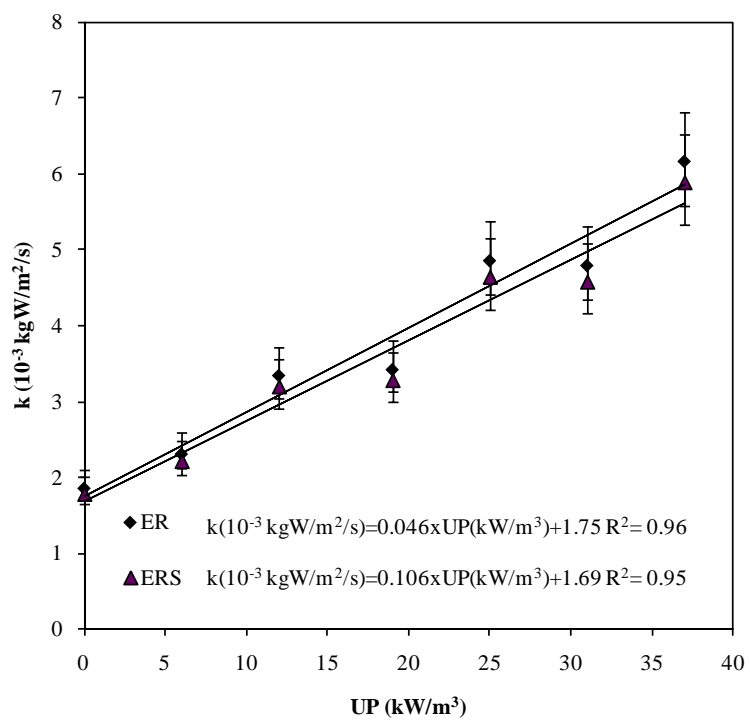
600

601 FIG 4. Influence of the ultrasonic power density (UP) on the mass transfer coefficient.

602 Average values \pm LSD intervals ($p < 0.05$).

603

604

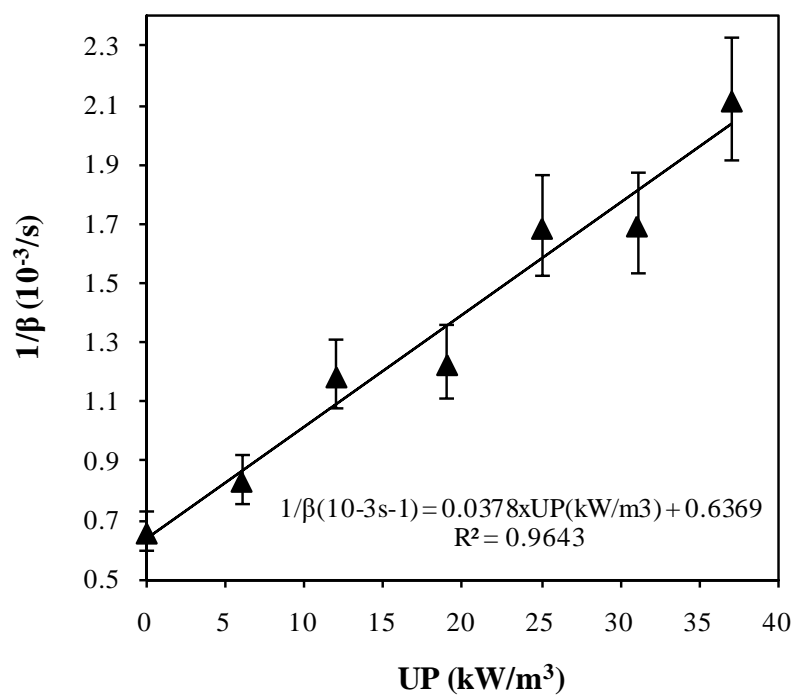


605

606 FIG 5. Influence of the ultrasonic power density (UP) on the mass transfer coefficient.

607 Average values \pm LSD intervals ($p < 0.05$).

608



609

610 FIG. 6. Influence of ultrasonic power density on kinetic parameter $1/\beta$ of eggplant cylinders at611 1 m/s. Average values \pm LSD intervals ($p < 0.05$).

612